Neutron irradiation impact on AlGaN/GaN HEMT switching transients

Peter A. Butler, Michael J. Uren, *Member, IEEE,* Benoit Lambert, and Martin Kuball, *Senior Member, IEEE*

***Abstract*—Current transient spectroscopy (CTS), was used to measure the impact of neutron irradiation on output current-limiting charge traps in AlGaN/GaN HEMTs with time constants from 10 ms to 1800 s. We find that coupling between discrete traps was apparent, in contrast to the commonly employed assumption of independent trap (dis)charging, and increased after 14 MeV neutron irradiation of 2×10^{13} n/cm^2 and above. Irradiation to a high dose of as much as 7.8×10^{14} n/cm^2, which is comparable to eight years exposure to a harsh radiation environment such as the ITER neutral beam injector prototype, increased trapped charge density, and reduced transient drain current to as little as 75% of its equilibrium value. These changes are consistent with displacement damage estimates based on radiation transport calculations.**

***Index Terms*—GaN, HEMT, 14 MeV neutron, switching transients, gate-lag, III-V semiconductors, displacement damage.**

I. Introduction

GALLIUM NITRIDE (GaN) High Electron Mobility Transistors (HEMTs) offer a combination of performance characteristics exceeding that available from competing technologies, making them prime candidates for use in future RF and power systems for harsh radiation environments. Aerospace applications demand tolerance of irradiation by neutrons with energies from thermal (25 meV), to hundreds of GeV in the case of neutrons generated by high energy primary cosmic rays [1]. 14 MeV neutron testing is representative of atmospheric Single Event Effects (SEE) environments in integrated and bipolar technologies [2], provided that the Linear Energy Transfer (LET) threshold is below 8 to 9 MeV cm^{-2} mg^{-1} [3], [4]. It has been suggested that GaN may be insensitive to single event gate rupture (SEGR) at these LET values [5]. Prototype electronic systems for future fusion power facilities, such as the International Thermonuclear Experimental Reactor (ITER [6]), will be exposed to 2.45 MeV and 14 MeV neutrons at fluences of up to 10^{14} n/cm^2 per year [7]. Reliable radiation-hardened electronics will be required for such future large-scale fusion devices [8]. Understanding AlGaN/GaN HEMT susceptibility to high fluence 14 MeV neutron irradiation is therefore a key step towards their insertion into nuclear fusion systems, and aids in understanding their performance in aerospace and other nuclear applications.

We consider here the cumulative displacement damage (DD) effects of neutron exposure on AlGaN/GaN HEMTs, rather than transient radiation or Single Event Effects (SEE). DD and non-ionising energy loss (NIEL) effects in semiconductors due to fast neutrons scattering from atoms in the lattice include the creation of point defects including vacancies, interstitials, Frenkel pairs and defect-impurity complexes, as reviewed for the case of silicon by Srour *et al* [9]. DD and NIEL effects are not only an important consideration for the nuclear environments mentioned above: space missions featuring proton-rich orbits also need to consider DD effects, for example the European Space Agency's JUICE mission to Europa will be exposed to 10^6 p$^+$ cm^{-2} sr^{-1} s^{-1} MeV^{-1} [10]. DD testing is typically performed for optoelectronics, sensors, and bipolar technologies. However, previous studies have shown that irradiation of AlGaN/GaN HEMTs with 2.8×10^{11} n/cm^2($\langle$E$\rangle = 9.8$ MeV) [11] can cause a 10% reduction in drain-source current (I_{DS}), and irradiation by 1.6×10^{12} n/cm^2 (1 MeV equivalent) [12] was found to cause increases in gate leakage current via trap-assisted tunnelling in the AlGaN gate region. A higher neutron fluence study found reductions in I_{DS} and transconductance (G_m), but not cut-off frequency after exposure to 10^{15} n/cm^2($\langle$E$\rangle = 1$ MeV) [13]. Conversely, AlGaN/GaN HEMTs degraded by prior electrical stress have shown partial recovery of I_{DS} [14] following irradiation with thermalised Am-Be neutrons to 6×10^{11} n/cm^2. Consequently, the impact of neutron irradiation on the switching and transient recovery characteristics of HEMTs remains unclear.

In this work we use current transient spectroscopy (CTS) to show that AlGaN/GaN HEMT switching transients are indeed sensitive to fast neutron irradiation. Whether the sensitivity produces a favourable change, such as a decrease in the time taken to switch from off-state to the desired on-state output current, or a deleterious change (e.g. the inverse), depends not only upon the neutron fluence, but also on the duration of off-state biasing applied prior to measuring the switching transient.

II. Experimental details

The devices used in this study were AlGaN/GaN HEMTs grown on SiC substrates, and packaged in Egide ceramic RF packages. They had a gate length of $L_G = 0.25$ μm, source-drain distance $L_{SD} = 2.75$ μm, and gate-drain distance $L_{GD} = 1.7$ μm. The HEMTs had eight 100 μm fingers. Threshold voltages were ≈ -3.3 V, and peak transconductance was 0.17 Siemens (213 mS/mm). Further information on these UMS GH25-10 devices can be found in [15].

Three HEMTs were irradiated at AWE's ASP accelerator [16], [17], where 14 MeV neutrons were generated

P.A. Butler, M.J. Uren, and M. Kuball are with the Centre for Device Thermography and Reliability, H. H. Wills Physics Laboratory, University of Bristol, United Kingdom. P.A.B. is also with AWE Plc., Aldermaston, Reading, United Kingdom. e-mail: Peter.Butler@Bristol.ac.uk

B. Lambert is with United Monolithic Semiconductors, Villebon Sur Yvette, France.

Manuscript received 26th July, 2018.

by deuterium-tritium (DT) fusion: the dominant reaction is ${}^{2}_{1}\mathrm{H} + {}^{3}_{1}\mathrm{H} => \mathrm{n} + {}^{4}_{2}\mathrm{He} + 17.62\ \mathrm{MeV}$. In this reaction the emitted alpha particle has energy $\mathrm{E}_{\alpha} = 3.5\ \mathrm{MeV}$, and the neutron has $\mathrm{E_n} = 14.1\ \mathrm{MeV}$. HEMTs were unpowered during irradiation, and stored in conducting foam to mitigate charging effects. Exposure was uniform across the HEMT surface ($< 1\%$ variation). Three HEMTs were irradiated to neutron fluences of $2.1 \times 10^{13}\ \mathrm{n/cm^2}$, $1.24 \times 10^{14}\ \mathrm{n/cm^2}$, and $7.82 \times 10^{14}\ \mathrm{n/cm^2}$. The average rate of irradiation was $4.3 \times 10^{13}\ \mathrm{n/cm^2/day}$ (ASP was operational for up to 8 hours per day). Due to safety controls in place for the handling of radioactive components, post-irradiation electrical testing was conducted 4 days after the maximum neutron fluence was reached. At least 10% of the fluence for the $7.82 \times 10^{14}\ \mathrm{n/cm^2}$ irradiation was due to 2.45 MeV neutrons from deuterium-deuterium (DD) fusion [18] because of deuterium build-up and tritium depletion in the ASP targets during operation.

The HEMTs were characterised before and after irradiation using drain current ($\mathrm{I_D}$) transient spectroscopy of gate-lag measurements. The first step in measuring each HEMT $\mathrm{I_D}$ transient was to apply an off-state trap filling bias of gate voltage ($\mathrm{V_G}$) = -10 V, drain voltage ($\mathrm{V_D}$) = 0.5 V using Keithley 4200 Semiconductor Characterisation System source-measure units. $\mathrm{V_G}$ was chosen to ensure that the channel would be fully pinched off even if the threshold voltage changed after irradiation. The duration of off-state bias applied prior to each on-state transient measurement, $\mathrm{t_{fill}}$, was varied from 10^{-2} s to 10^{2} s in decade steps, enabling investigation of the filling time dependence of trap occupancy. Next, HEMTs were switched to $\mathrm{V_G} = 0$ V, $\mathrm{V_D} = 0.5$ V for 1800 s to measure the on-state $\mathrm{I_D}$ transient in the linear regime of operation. Measurement stage temperature was maintained at $25°\mathrm{C}$ throughout the testing. Prior to each measurement, a bias of $\mathrm{V_G} = 0.7$ V, $\mathrm{V_D} = 0$ V was applied to the devices for 10 minutes, resetting devices sufficiently for repeatable $\mathrm{I_D}$ transients.

III. Current Transient Spectroscopy

The two-dimensional electron gas (2DEG) density in the HEMT channel varies with the position of the Fermi level, polarisation, and the occupation of surface donors [19], barrier traps, and buffer traps. During off-state biasing potential gradients exist that cause electrons to be injected into available states in surface regions. This produces a virtual gate [20], [21], [22], shown extending from $\mathrm{W_1}$ to $\mathrm{W_2}$ in Figure 1-**a**. The -10 V bias applied to the gate during $\mathrm{t_{fill}}$ was below the threshold voltage of the HEMTs, and so also fully depleted the 2DEG under the gate and depleted the bulk (Al)GaN vertically and laterally to generate a screening charge. Bulk trapping of charge injected from the gate is likely in those regions (dark shading in Fig. 1-**a**). The lateral extent of the depletion into the drain and source access regions was estimated to be 100 nm using TCAD drift-diffusion simulation assuming a (unknown) background donor density of $5 \times 10^{16}\ \mathrm{cm^{-3}}$ (Silvaco Atlas) [23], giving a channel length probed by the off-state pulse, $\mathrm{L_P}$ of $\approx 0.45\ \mu$m. On-state biasing enabled redistribution of the trapped charge, and recovery of the 2DEG density in the HEMT channel.

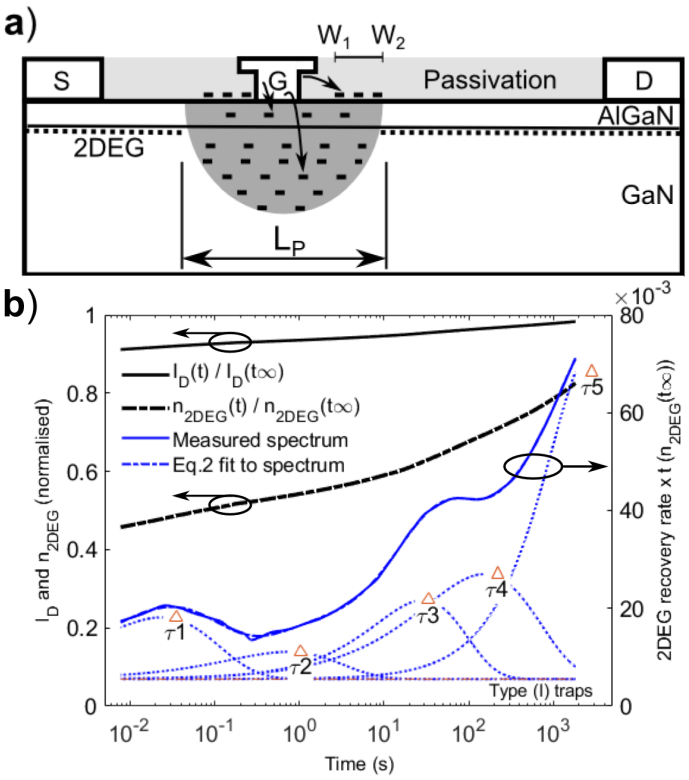

Fig. 1. **a**) Schematic of a lateral HEMT used in this work. Negative charge trapped by off-state bias depletes the 2DEG within $\mathrm{L_P}$. Trap locations shown for Type (I) traps (likely in the passivation layer, passivation/AlGaN surface, AlGaN barrier); and Type (II) traps (dominant in GaN bulk). **b**) un-irradiated HEMT normalised $\mathrm{I_D(t)}$ for $\mathrm{t_{fill}} = 100$ s, corresponding normalised $\mathrm{n_{2DEG}(t)}$, and detrapping spectrum fit using five Type (II) trap terms.

Conventionally, HEMT transient current at time t, $\mathrm{I_D(t)}$, is used directly to produce a detrapping spectrum to measure relative trap densities and activation energies by employing an underlying assumption that the transients depend on multiple independent trapping processes [24], [25], [26]. However, because the off-state bias will only change the charge state of traps located within the depletion region under the gate (Fig. 1-**a**), using this approach will underestimate the change in channel charge density there. In series with the intrinsic transistor and source/drain access resistances are drain and source contact resistances ($2\mathrm{R_C}$), and because a two-wire measurement was used, cable resistance must also be considered by setting a total extrinsic resistance, $\mathrm{R_{ext}} = 2\mathrm{R_C} + \mathrm{R_{cables}}$. For the HEMTs tested here, $\mathrm{R_{ext}}$ was similar to the channel resistance at 10^4 s, and so cannot be ignored. We normalised $\mathrm{I_D(t)}$ by the maximum extrapolated drain current reached at 10^4 s following an off-state pulse $\mathrm{I_D(t\infty)}$. By utilising the length of the depletion region $\mathrm{L_P}$, the channel length $\mathrm{L_{SD}}$, and the extrinsic resistance $\mathrm{R_{ext}}$, an equation was derived for the non-linear relationship between 2DEG density within the region probed by the off-state pulse and the measured current:

$$\mathrm{n_{2DEG}(t)} = \frac{\mathrm{I_{norm}(t)\,L_P\,n_{2DEG}(t=\infty)}}{\mathrm{R^*(1-I_{norm}(t)) + I_{norm}(t)(L_P - L_{SD}) + L_{SD}}} \quad (1)$$

where $\mathrm{I_{norm}(t)} = \frac{\mathrm{I_D(t)}}{\mathrm{I_D(t\infty)}}$, and

$R^* = R_{ext}\, W\, \mu\, q\, n_{2DEG}\,(t = \infty)$. W is total HEMT width, μ is mobility and taken as 1400 cm^2/Vs, and q is the electronic charge. Figure 1-**b** shows the non-linear relationship between $I_{norm}(t)$ and $n_{2DEG}(t)$, demonstrating that local changes in n_{2DEG} are much larger than the measured change in I_D.

Transient spectra were produced by differentiating $\frac{n_{2DEG}(t)}{n_{2DEG}(t\infty)}$ with respect to $\log_e(t)$ (equivalent to t x 2DEG density recovery rate), then plotting against $\log_{10}(t)$, as shown in Fig.1-**b**. Efficacy of 2DEG depletion varies with trapped charge location [27] depending on whether its image charge resides completely in the channel or also resides partially in the metal contacts, hence the integrated recovery rate is the effective trapped charge emitted during the integration period. This enables semi-quantitative analysis of trap densities from I_D current transients.

To analyse the spectra we consider transient n_{2DEG} changes due to I) traps with a continuously varying time constant within the limits of the measurement, and II) traps with discrete time constants. A constant density of traps over some range of tunnelling distances from the gate (W1 to W2 as shown in Fig.1-**a**), with time constants that lie within the measurement window, will exhibit charge capture or emission current decreasing with time as 1/t [28], i.e. : $dn_{trapped}(t)/dt = n_{trapped}(t_0)/t$ (Type (I) traps). This appears as a constant baseline on the I_D transient spectra. Conversely, such a distribution of slow traps can also cause noise that decreases with frequency i.e. flicker (1/f) noise [29] due to carrier number fluctuations. Application of the Dutta-Horn model [30] to 1/f noise in GaN has been used to estimate the defect energy distributions in GaN devices [31], [32]. The slow traps responsible for these effects could be located in the passivation, or on the surface forming a virtual gate, or in the AlGaN barrier. Trapped charge current to/from Type (II) traps, assumed to be primarily located in the bulk GaN, was considered using stretched exponential functions [33], [26]. This treatment is appropriate for independent traps such as non-interacting point defects, and for clusters of traps, including those generated by energetic displacement damage cascades, where trap depth is modified by an occupancy dependent Coulomb potential. Active trap density (effective density acting within the measurement time window), and time constants were found by fitting each spectrum with the function:

$$\frac{\partial n_{2DEG}(t)}{\partial \ln(t)} = A + \Sigma_{i=1}^{N} D_i\, e^{\left(-\frac{t}{\tau_i}\right)^{\beta_i}} \qquad (2)$$

where A is the effective charge density at the start of the transient (t_0) in Type (I) traps. The summation term represents charge emission from N Type (II) traps. τ_i is the emission time constant of each discrete trap. $D_i = \beta_i\, n_{trapped,i}(t_0)\left(\frac{t}{\tau_i}\right)^{\beta_i}$, where $n_{trapped,i}$ is the normalised effective charge density in the i^{th} discrete trap and β_i is the stretch parameter which can vary from 1.0 to 0.6 in our fit. Decreasing β below 1 increases the proportion of detrapping occurring after the peak in the $\frac{\partial n_{2DEG}(t)}{\partial ln(t)}$ function, therefore an average time constant [34] is used to describe stretched exponential traps: $< \tau >= \frac{\tau}{\beta}\Gamma\left(\frac{1}{\beta}\right)$. An example fit with five discrete traps and a continuum is shown in Fig.1-**b**.

IV. Results

Transient drain current, $I_D(t)$, increased quasi-linearly with the logarithm of measurement time for all tested HEMTs prior to irradiation, as shown in Figs 2-**a**, -**b**, and -**c**, with little device-to-device variation in the extent of the I_D increase observed during the transients or its t_{fill} dependence. Increasing trap filling time, t_{fill}, caused a small reduction of $I_D(t)$ from $t = 10^{-1}$ s to $t > 1.8 \times 10^3$ s, indicating a small increase in effective density of negative trapped charge in the HEMTs. We note that at times less than $t = 10^{-1}$ s, $I_D(t)$ varied non-monotonically with t_{fill}, increasing until $t_{fill} = 1$ s, then decreasing for larger t_{fill} values, suggesting the presence of discrete traps responding more quickly than the shortest measurement times. One second after switching to the on-state (t = 1 s), the mean $I_D(t)$ was $(95 \pm 1)\%$ of $I_D(t\infty)$.

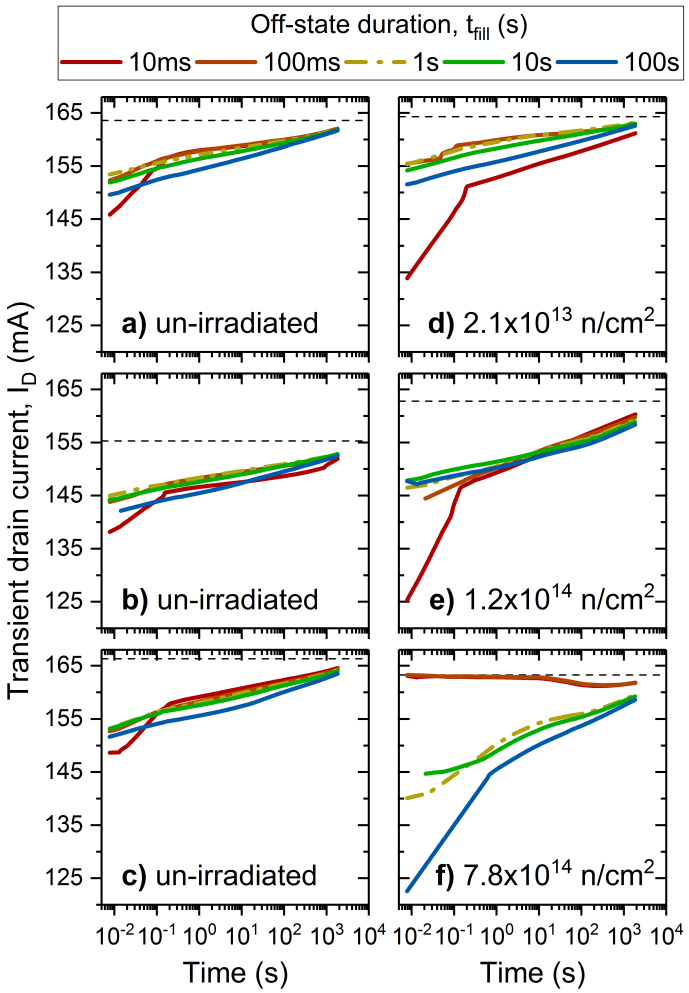

Fig. 2. Drain current transients after t_{fill} of 10 ms to 100 s in decade steps, prior to irradiation (**a**, **b**, **c**), and for corresponding HEMTs following neutron irradiation to fluences of: 2.1×10^{13} n/cm^2 (**d**), 1.2×10^{14} n/cm^2 (**e**), and 7.8×10^{14} n/cm^2 (**f**). The dashed lines indicate $I_D(t\infty)$.

After irradiation, HEMT $I_D(t)$ sensitivity to changes of t_{fill} had increased, as is apparent in Figs.2-**d**, -**e**, and -**f**. Averaged over the three irradiation levels, mean $I_D(t)$ at t = 1 s was

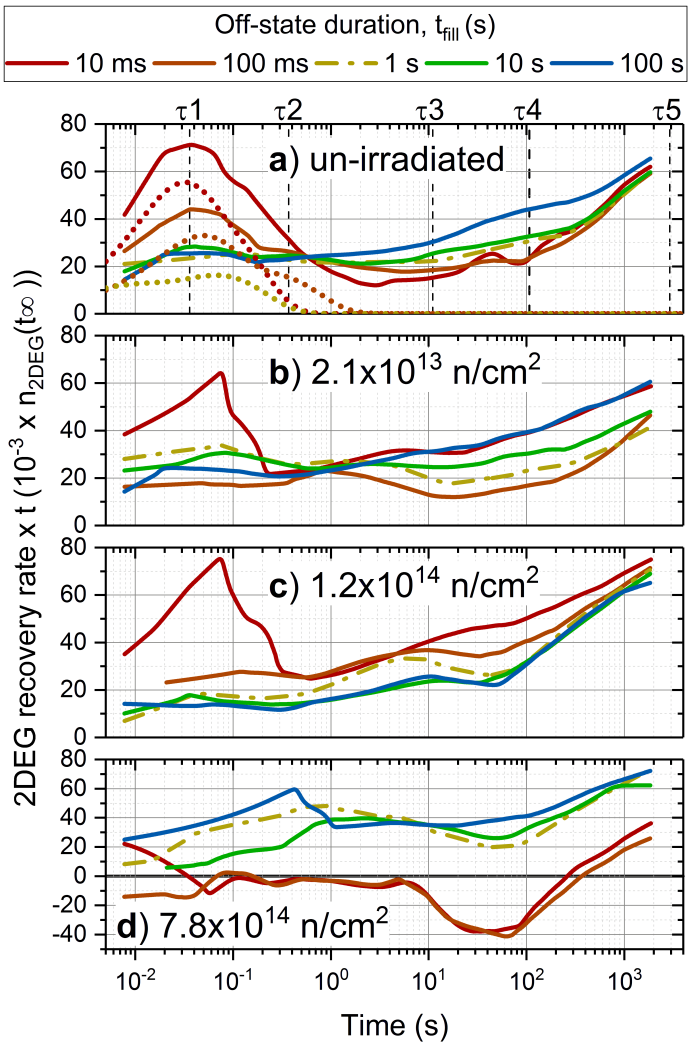

Fig. 3. Measured transient spectra for all t_{fill} values before irradiation (**a**), and as a function of increasing neutron fluence: (**b**), (**c**), and (**d**). The time constants for the five fitted Type (II) traps are shown. To fit the 10 ms and 100 ms spectra in (**d**) required a negative baseline. Dotted coloured lines in **a** show the sum of the fitted $\tau 1 + \tau 2$ components for $t_{fill} = 10$ ms, 100 ms, and 1s. **a** and **b** are the same device before and after irradiation.

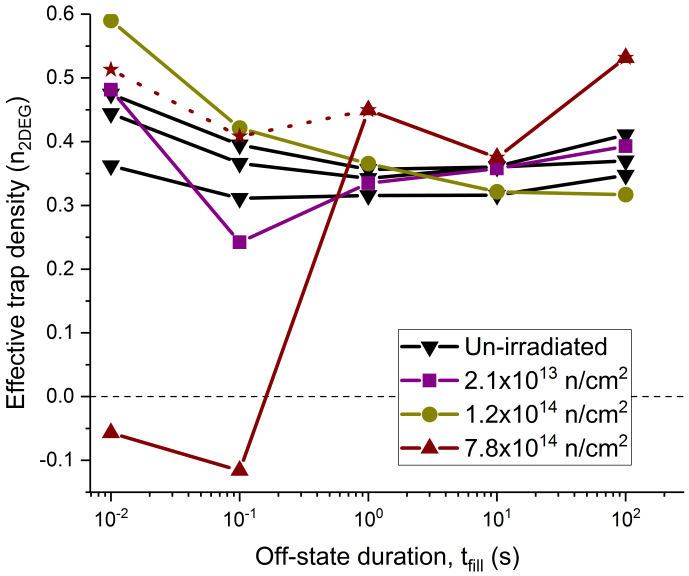

Fig. 4. Effective density of trapped negative charge within the depletion region emitted during the measurement, plotted against off-state duration as a function of neutron fluence. Densities were found by integrating fits of the 2DEG recovery rates of the depletion region in Fig. 3. Starred points connected by dots show the maximum fluence case after subtracting the positive charge emission found by fitting Eq. 2. Connecting lines are a guide to the eye.

$(94 \pm 2)\%$ of $I_D(t\infty)$. Transients measured after irradiation to a fluence of 7.8×10^{14} n/cm^2 are displayed in Fig. 2-**f**: for $t_{fill} = 100$ s, I_D at the start of the transient was 75% of $I_D(t\infty)$, whereas prior to irradiation (Fig. 2-**c**), it was 91%, suggesting an irradiation-induced increase in effective negative trapped charge density.

Five Type (II) trap terms labelled $\tau 1 : \tau 5$, were required for a satisfactory fit of Eq. 2 to the experimental data. These traps were enhanced by irradiation, obscuring, and in some cases suppressing the Type I traps with an apparent continuum of time constants. Time constants for traps $\tau 1 : \tau 5$ for the un-irradiated HEMT transients were: $\tau 1 = 0.036 \pm 0.013$ s, $\tau 2 = 0.37 \pm 0.24$ s, $\tau 3 = 11 \pm 9$ s, $\tau 4 = 107 \pm 43$ s, and $\tau 5 = 2910 \pm 1117$ s (see Figs1-**b** and 3-**a**). The large error suggests that this is not a unique trap attribution, however it provides a valuable means of comparing and analysing responses.

Figure 3 illustrates how the effect of increasing t_{fill} on transient spectra depends on neutron exposure. Prior to irradiation (Fig. 3-**a**), increasing t_{fill} above one second monotonically increased the 2DEG recovery rate observed for $t \geq 1$ s during the transient measurements for all tested HEMTs. Changes in the HEMT transient recovery rate and t_{fill} dependence are clearly apparent after irradiation (Figs 3-**b**, -**c**, and -**d**). However, the trend is not fully clear, especially given that only one HEMT could be tested at each neutron fluence.

The normalised active density of all traps in the 10^{-2} to 10^3 s time window ($\tau 1 : \tau 5$ and the continuum trap) was found by fitting Eq. 2 to the experimental data in Fig. 3 and integrating under the curves. This is plotted in Fig. 4. For the un-irradiated devices, increasing t_{fill} from 10^{-2} s to 1 s lowered the total active trap density by reducing the combined $\tau 1$ and $\tau 2$ contributions. A total active trapped charge density of $\approx 0.38\ n_{2DEG}(t\infty)$ was approached at high t_{fill}. After irradiation, maximum active trap density increased, as did the maximum change in active density obtained by varying t_{fill} (the range). For the 7.8×10^{14} n/cm^2 case, net positive charge emission was apparent during the $t_{fill} = 10$ ms and 100 ms transients.

The DC drain-source current (I_{DS}) and gate-source current (I_{GS}) characteristics for the HEMTs are shown in Figure 5 for each of the un-irradiated and irradiated cases. Curves were measured using double V_{GS} sweeps (reverse then forward). Following irradiation changes were present in the magnitude and the hysteresis of the I_{DS} curves, suggesting altered trapping behaviour, as shown in the figure. However, a clear trend is not apparent in the DC measurement results.

V. Damage Modelling

Radiation transport calculations [35] using the Monte Carlo particle radiation transport code MCNP6 [36], show that differences in the number and energy spectra of primary knock-on

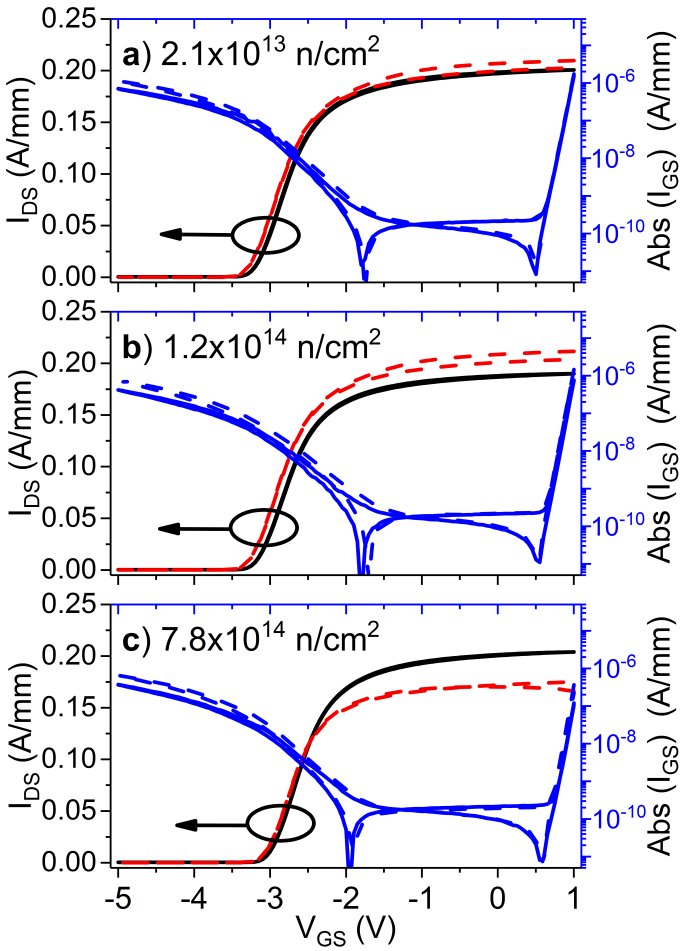

Fig. 5. Drain-source current (I_{DS}) and gate-source current (I_{GS}) each normalised by gate width ($W_G = 800\ \mu m$), are shown plotted against gate-source voltage (V_{GS}). Drain-source voltage was $V_{DS} = 0.5V$. **a**), **b**), and **c**) show un-irradiated (solid lines), and corresponding irradiated (dashed lines) characteristics for each HEMT.

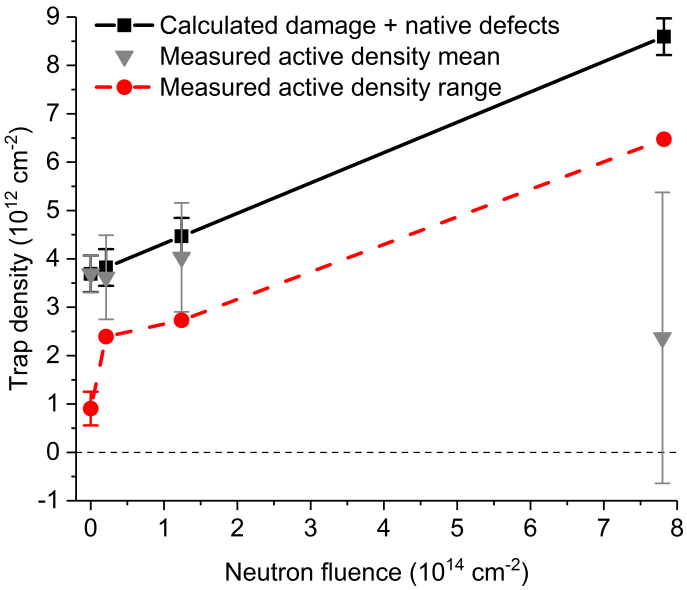

Fig. 6. Sum of calculated irradiation-induced stable defect density and measured native density against neutron fluence. The active trap density in the depletion region, and the maximum change in active density by varying t_{fill} (the range), found by fitting Eq. 2 to the current transient spectra and assuming a nominal $n_{2DEG}(t\infty) = 10^{13}\ cm^{-2}$ are shown for comparison. Connecting lines are a guide to the eye.

atoms (PKAs) produced in the HEMT semiconductor regions due to 14 MeV DT neutrons and 2.45 MeV DD neutrons are minimal. The variation in the incident neutron energy spectrum with time can therefore be disregarded in the present work. PKA density was calculated to be between 1×10^{-7} and $8 \times 10^{-7}\ cm^{-2}/(n/cm^2)$, with the highest densities expected in the gate-drain and gate-source access regions due to higher energy PKAs from the SiN passivation entering the barrier.

We estimate the resulting stable defect densities by using the modified Kinchin-Pease model [37] and setting mean damage energy equal to the calculated primary recoil energy in each spectrum division. Defect densities calculated in this work are for indication only because of the inherent difficulties involved [9] when considering displacement damage in binary and ternary alloys with widely differing atomic numbers and the uncertain influence of clustering at the high peak PKA energies considered (MeV). The calculated defect densities under the gate are $2.81 \times 10^{-4}\ cm^{-2}/(n/cm^2)$ in AlGaN and $3.77 \times\ 10^{-3}\ cm^{-2}/(n/cm^2)$ in GaN. In the access regions, defect densities of $4.53 \times 10^{-3}\ cm^{-2}/(n/cm^2)$ in AlGaN and $4.52 \times 10^{-7}\ cm^{-2}/(n/cm^2)$ in GaN were calculated. The expected stable defect densities within the HEMT depletion regions, as plotted in Fig.6, were calculated using these values and setting $n_{2DEG}(t\infty) = 10^{13}\ cm^{-2}$.

By assuming that all calculated defects within the region bounded by L_P and extending throughout the GaN buffer are electrically active, we find that three HEMT regions, 1) the AlGaN in the access regions on the source and drain sides of the gate, 2) the bulk GaN in the access regions, and 3) the GaN under the gate, would each trap approximately one third of the measured trapped charge. Surprisingly, only around 3% of the trapped charge would be stored in the AlGaN under the gate. GaN buffer defects would therefore account for around two thirds of the measured traps.

Considering the nature of this calculation, it is encouraging that the measured active trap densities, and their range probed by varying t_{fill}, are less than, but broadly comparable to, the defect densities expected from the damage modelling (Fig.6). It is possible that the trapped charge changes following irradiation are due to changes in pre-existing traps, however this calculation confirms that the trap density changes can plausibly be attributed to displacement damage.

VI. Discussion

There is little device-to-device variation in trapping observed using drain current transient spectroscopy prior to neutron irradiation (Figs. 2, 4, 6). The measured active trap density range found by varying t_{fill} was $(9.0 \pm 3.5) \times 10^{11}\ cm^{-2}$ prior to irradiation; it more than doubled to $2.4 \times 10^{12}\ cm^{-2}$ after irradiation to $2.1 \times 10^{13}\ n/cm^2$, and increased further with increasing neutron fluence. The HEMT 2DEG channel density transients, $n_{2DEG}(t)$, calculated from $I_D(t)$ by accounting for the limited depletion region contribution to the

extrinsic HEMT drain-source resistance, are reasonably well fitted using Eq. 2, suggesting that the model is credible.

Damage constants for mobility reduction due to displacement damage in compound semiconductors are expected to be several orders of magnitude lower than for carrier lifetime reduction [38]. Therefore we expect that neutron-induced mobility reduction is not significant in our results. This assumption is supported by the small changes to the measured late time current after irradiation (Fig. 2, dashed lines).

There is an expectation that Type (II) trap occupancy depends exponentially on t_{fill} under low trapping conditions, or has a logarithmic t_{fill} dependence under high trapping conditions [39]. However, the sum of the active density of $\tau 1$ plus $\tau 2$ in the un-irradiated HEMTs decreased as t_{fill} was increased from 10 ms to 1 s, shown by the dotted coloured lines in Fig. 3-**a**; whereas the active density of slower traps ($\tau 3$, $\tau 4$, and $\tau 5$), increased monotonically with increasing t_{fill}. Total active trap densities (Fig. 4), show a non-monotonic dependence on t_{fill}. This is surprising since active trap density is a function of occupancy, and should therefore increase or saturate with increasing t_{fill}, but not decrease. This observation can be explained if trap occupancies are coupled. A mechanism for trap coupling would be charge migrating to more energetically favourable locations during long periods of off-state biasing: either to traps with time constants outside the measurement range, or to regions where it is less effective at depleting n_{2DEG} (e.g. migrating from the GaN buffer, where the 2DEG is the only screening conductor, to the AlGaN barrier under the gate where image charge will partially reside on the gate). Here we note that two distinct peaks in an I_D transient spectrum can also be caused by two rate limiting conduction pathways from a single trap [40]. Given the apparent coupling and lack of straightforwardly extractable time constants, it is not possible to attribute the defects to those listed in papers such as [26], [32].

After irradiation the active density of all traps displayed a non-monotonic dependence on t_{fill} (Fig. 3-**b**, -**c**, and -**d**), with the resulting overall increase in coupling and device-to-device variation apparent in Fig. 4. Maximum active densities also increased after irradiation to a fluence of 1.2×10^{14} n/cm^2 and above. This could be caused by displacement damage affecting conduction pathways by altering the potential distribution in the bulk as it charges, or by enhancing inter-trap coupling because of its increased density. The baseline of Type (I) traps was suppressed for the highest irradiation level (where calculated damage density exceeded native trap density) followed by measurement at short fill times (Fig. 2-**f**). This suggests that either 1) Type (I) traps were actually a superposition of discrete traps, and irradiation caused the traps to change to respond outside the measurement time window or 2) the continuum trap was screened by the enhanced charge in Type (II) traps, i.e. another coupling mechanism. The increased range of active trap density achievable by varying t_{fill} after irradiation (Fig. 6), could be due to coupling to traps with time constants outside the measurement window, and an increased density of traps with time constants within the measurement window, as expected from displacement damage calculations.

Iron (Fe) doping is used in these devices to achieve semi-insulating GaN buffers and to eliminate punch-through effects [41]. This is known to make GaN n-type, unless excess carbon renders the GaN p-type [42], although other intrinsic defects such as vacancies and interstitials are likely to be present and would contribute to the effective doping. Bardeleben et al. [43] found that particle irradiation can generate a split nitrogen interstitial defect (ambipolar, acting as a deep acceptor at $E_c - 1.0$ eV in n-type GaN and as a deep donor in p-type GaN), at a rate close to that of the generation of nitrogen interstitials (acceptors in n-GaN [44]). In p-type GaN the nitrogen vacancy, a donor, has the lowest formation energy [45], whereas in n-type GaN the gallium vacancy is most likely and acts as an acceptor. The net effect of these defects is likely to increase the intrinsic nature of the GaN by compensation, thus reducing conductivity, although hopping conduction can lead to an increase in leakage current under reverse bias . These mechanisms are illustrated in Fig. 7-**a** for band-edge transport where a net increase in trapped negative charge occurs. Donors, which are positioned deep in the buffer, are neutralised by electron capture, and holes are emitted by acceptors. In Fig. 7-**b** trapped negative charge is shown to be emitted into the channel and gate by ionising deep donors and by hole current flowing into the buffer. Therefore, it is plausible that displacement damage defects, the approximate densities of which were given above, are responsible for the observed changes in HEMT switching and transient recovery characteristics.

The transient recovery of HEMT output current following off-state biasing has a complex dependence on biasing conditions after irradiation: changes can vary from an apparent complete suppression to a major enhancement of active trap density, increasing gate lag and resulting in slower overall I_D recovery. This demonstrates that AlGaN/GaN HEMT neutron damage susceptibility is more complex at these irradiation levels than suggested by previous reports of either neutron-induced defect suppression [14], or output degradation [11], [13].

VII. Conclusions

We have shown that despite the well-known comparative insensitivity of AlGaN/GaN HEMT DC characteristics to neutron irradiation, 14 MeV neutron irradiation of 2×10^{13} n/cm^2 and beyond can alter the magnitude and duration of AlGaN/GaN HEMT switching transients, due to increases in inter-trap coupling and trap density. We find the recovery rate of 2DEG density, and therefore drain current, following off-state to on-state switching can decrease or increase after irradiation, depending in a complex manner on trap filling conditions, and merits further research. Simulations of HEMT performance after irradiation based on testing a small set of biasing conditions and using simple charge trapping models such as Eq. 2 are unlikely to capture the complex emergent trap coupling behaviour we have observed. Since this behaviour is an important consideration in circuit applications, HEMT transient characteristics should be considered in addition to DC parameters when assessing and certifying components for use in harsh neutron radiation environments.

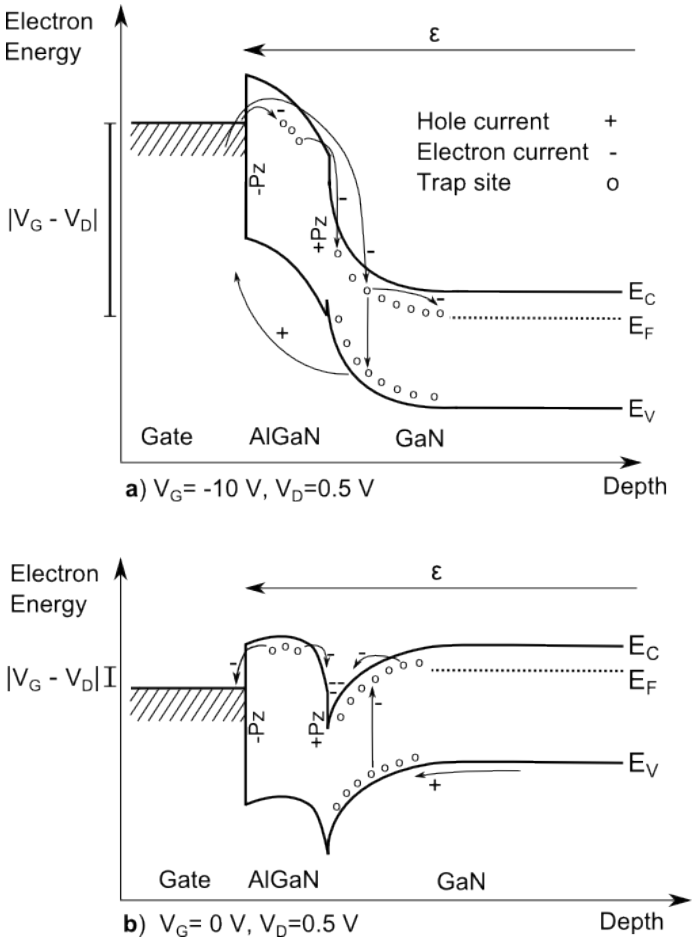

Fig. 7. Band diagrams showing charge (de)trapping currents for the region under the HEMT gate during: (**a**) off-state, and (**b**) on-state biasing.

ACKNOWLEDGMENTS

This work was supported by the AWE Technical Outreach Fund. We are grateful to the AWE ASP accelerator team and to Verity Woolhead (AWE) for support with performing irradiations. We thank Dr James Pottage (AWE) for radiation transport calculations, and Dr Hareesh Chandrasekar (UoB) for TCAD calculations, and Dr Máire Power (Nu Nano Ltd) for helpful comments on the manuscript.

REFERENCES

[1] C. Dyer, A. Hands, K. Ford, A. Frydland, and P. Truscott, "Neutron-Induced Single Event Effects Testing Across a Wide Range of Energies and Facilities and Implications for Standards," *IEEE Trans. Nucl. Sci.*, vol. 53, no. 6, pp. 3596–3601, Dec 2006.

[2] E. Normand and L. Dominik, "Cross Comparison Guide for Results of Neutron SEE Testing of Microelectronics Applicable to Avionics," in *2010 IEEE Radiation Effects Data Workshop*, July 2010, pp. 50–57.

[3] F. Irom, T. F. Miyahira, D. N. Nguyen, I. Jun, and E. Normand, "Results of Recent 14 MeV Neutron Single Event Effects Measurements Conducted by the Jet Propulsion Laboratory," in *2007 IEEE Radiation Effects Data Workshop*, July 2007, pp. 141–145.

[4] C. Weulersse, N. Guibbaud, A. L. Beltrando, J. Galinat, C. Beltrando, F. Miller, P. Trochet, and D. Alexandrescu, "Preliminary Guidelines and Predictions for 14-MeV Neutron SEE Testing," *IEEE Trans. Nucl. Sci.*, vol. 64, no. 8, pp. 2268–2275, Aug 2017.

[5] S. Bazzoli, S. Girard, V. Ferlet-Cavrois, J. Baggio, P. Paillet, and O. Duhamel, "SEE sensitivity of a COTS GaN transistor and silicon MOSFETs," in *9th European Conference on Radiation and Its Effects on Components and Systems*, Sept 2007.

[6] What is ITER? [Online]. Available: https://www.iter.org/proj/inafewlines

[7] M. Bagatin, A. Coniglio, M. D'Arienzo, A. D. Lorenzi, S. Gerardin, A. Paccagnella, R. Pasqualotto, S. Peruzzo, and S. Sandri, "Radiation Environment in the ITER Neutral Beam Injector Prototype," *IEEE Trans. Nucl. Sci.*, vol. 59, no. 4, pp. 1099–1104, Aug 2012.

[8] J. L. Bourgade, A. E. Costley, R. Reichle, E. R. Hodgson, W. Hsing, V. Glebov, M. Decreton, R. Leeper, J. L. Leray, M. Dentan, T. Hutter, A. Moroo, D. Eder, W. Shmayda, B. Brichard, J. Baggio, L. Bertalot, G. Vayakis, M. Moran, T. C. Sangster, L. Vermeeren, C. Stoeckl, S. Girard, and G. Pien, "Diagnostic components in harsh radiation environments: Possible overlap in R&D requirements of inertial confinement and magnetic fusion systems," *Review of Scientific Instruments*, vol. 79, no. 10, p. 10F304, 2008. [Online]. Available: https://doi.org/10.1063/1.2972024

[9] J. R. Srour, C. J. Marshall, and P. W. Marshall, "Review of displacement damage effects in silicon devices," *IEEE Trans. Nucl. Sci.*, vol. 50, no. 3, pp. 653–670, June 2003.

[10] D. Lasi, M. Tulej, S. Meyer, M. Lthi, A. Galli, D. Piazza, P. Wurz, D. Reggiani, H. Xiao, R. Marcinkowski, W. Hajdas, A. Cervelli, S. Karlsson, T. Knight, M. Grande, and S. Barabash, "Shielding an MCP Detector for a Space-Borne Mass Spectrometer Against the Harsh Radiation Environment in Jupiter's Magnetosphere," *IEEE Trans. Nucl. Sci.*, vol. 64, no. 1, pp. 605–613, Jan 2017.

[11] B.-J. Kim, H.-Y. Kim, J. Kim, and S. Jang, "Neutron irradiation on AlGaN/GaN high electron mobility transistors on SiC substrates," *Journal of Crystal Growth*, vol. 326, no. 1, pp. 205 – 207, 2011, symposium on Wide Bandgap Semiconductors (III-Nitrides, SiC, and Diamond). [Online]. Available: http://www.sciencedirect.com/science/article/pii/S0022024811001497

[12] J. C. Petrosky, J. W. McClory, T. E. Gray, and T. A. Uhlman, "Trap Assisted Tunneling Induced Currents in Neutron Irradiated AlGaN/GaN HFETs," *IEEE Trans. Nucl. Sci.*, vol. 56, no. 5, pp. 2905–2909, Oct 2009.

[13] L. Ling, Z. Jin-Cheng, X. Jun-Shuai, M. Xiao-Hua, Z. Wei, B. Zhi-Wei, Z. Yue, and H. Yue, "Neutron irradiation effects on AlGaN/GaN high electron mobility transistors," *Chinese Physics B*, vol. 21, no. 3, p. 037104, 2012. [Online]. Available: http://stacks.iop.org/1674-1056/21/i=3/a=037104

[14] F. Berthet, S. Petitdidier, Y. Guhel, J. L. Trolet, P. Mary, C. Gaquire, and B. Boudart, "Influence of Neutron Irradiation on Electron Traps Existing in GaN-Based Transistors," *IEEE Trans. Nucl. Sci.*, vol. 63, no. 3, pp. 1918–1926, June 2016.

[15] D. Floriot, V. Brunel, M. Camiade, C. Chang, B. Lambert, Z. Ouarch-Provost, H. Blanck, J. Grnenptt, M. Hosch, H. Jung, J. Splettster, and U. Meiners, "Gh25-10: New qualified power gan hemt process from technology to product overview," in *2014 9th European Microwave Integrated Circuit Conference*, Oct 2014, pp. 225–228.

[16] N. Bainbridge, "ASP particle accelerator," *AWE Discovery Journal*, 2004.

[17] L. Packer, M. Gilbert, S. Hughes, S. Lilley, R. Pampin, and J.-C. Sublet, "Uk fusion technology experimental activities at the asp 14mev neutron irradiation facility," *Fusion Engineering and Design*, vol. 87, no. 5, pp. 662 – 666, 2012, tenth International Symposium on Fusion Nuclear Technology (ISFNT-10). [Online]. Available: http://www.sciencedirect.com/science/article/pii/S0920379612000555

[18] T. Guymer, private communication, 2016.

[19] J. P. Ibbetson, P. T. Fini, K. D. Ness, S. P. DenBaars, J. S. Speck, and U. K. Mishra, "Polarization effects, surface states, and the source of electrons in AlGaN/GaN heterostructure field effect transistors," *Applied Physics Letters*, vol. 77, no. 2, pp. 250–252, 2000. [Online]. Available: https://doi.org/10.1063/1.126940

[20] S. C. Binari, K. Ikossi, J. A. Roussos, W. Kruppa, D. Park, H. B. Dietrich, D. D. Koleske, A. E. Wickenden, and R. L. Henry, "Trapping effects and microwave power performance in AlGaN/GaN HEMTs," *IEEE Transactions on Electron Devices*, vol. 48, no. 3, pp. 465–471, Mar 2001.

[21] G. Koley, V. Tilak, L. F. Eastman, and M. G. Spencer, "Slow transients observed in AlGaN/GaN HFETs: effects of SiNx passivation and UV illumination," *IEEE Transactions on Electron Devices*, vol. 50, no. 4, pp. 886–893, April 2003.

[22] A. Wells, M. Uren, R. Balmer, K. Hilton, T. Martin, and M. Missous, "Direct demonstration of the virtual gate mechanism for current collapse in AlGaN/GaN HFETs," *Solid-State Electronics*, vol. 49, no. 2, pp. 279 – 282, 2005. [Online]. Available: http://www.sciencedirect.com/science/article/pii/S0038110104003119

[23] H. Chandrasekar, private communication, 2018.

[24] M. Tapajna, R. J. T. Simms, Y. Pei, U. K. Mishra, and M. Kuball, "Integrated Optical and Electrical Analysis: Identifying Location and Properties of Traps in AlGaN/GaN HEMTs During Electrical Stress," *IEEE Electron Device Letters*, vol. 31, no. 7, pp. 662–664, July 2010.

[25] J. Joh and J. A. del Alamo, "A Current-Transient Methodology for Trap Analysis for GaN High Electron Mobility Transistors," *IEEE Transactions on Electron Devices*, vol. 58, no. 1, pp. 132–140, Jan 2011.

[26] D. Bisi, M. Meneghini, C. de Santi, A. Chini, M. Dammann, P. Brckner, M. Mikulla, G. Meneghesso, and E. Zanoni, "Deep-Level Characterization in GaN HEMTs-Part I: Advantages and Limitations of Drain Current Transient Measurements," *IEEE Transactions on Electron Devices*, vol. 60, no. 10, pp. 3166–3175, Oct 2013.

[27] O. Mitrofanov and M. Manfra, "Mechanisms of gate lag in gan/algan/gan high electron mobility transistors," *Superlattices and Microstructures*, vol. 34, no. 1, pp. 33 – 53, 2003. [Online]. Available: http://www.sciencedirect.com/science/article/pii/S0749603604000035

[28] R. H. Kingston and A. L. McWhorter, "Relaxation Time of Surface States on Germanium," *Physical Review*, vol. 103, pp. 534–540, Aug. 1956.

[29] A. Van Der Ziel, "On the noise spectra of semiconductor noise and of flicker effect," *Physica*, vol. 16, no. 4, pp. 359 – 372, 1950. [Online]. Available: http://www.sciencedirect.com/science/article/pii/0031891450900784

[30] P. Dutta and P. M. Horn, "Low-frequency fluctuations in solids: $\frac{1}{f}$ noise," *Rev. Mod. Phys.*, vol. 53, pp. 497–516, Jul 1981. [Online]. Available: https://link.aps.org/doi/10.1103/RevModPhys.53.497

[31] D. M. Fleetwood, "$1/f$noise and defects in microelectronic materials and devices," *IEEE Trans. Nucl. Sci.*, vol. 62, no. 4, pp. 1462–1486, Aug 2015.

[32] R. Jiang, X. Shen, J. Fang, P. Wang, E. X. Zhang, J. Chen, D. M. Fleetwood, R. D. Schrimpf, S. W. Kaun, E. C. H. Kyle, J. S. Speck, and S. T. Pantelides, "Multiple defects cause degradation after high field stress in algan/gan hemts," *IEEE Transactions on Device and Materials Reliability*, vol. 18, no. 3, pp. 364–376, Sept 2018.

[33] M. Meneghini, I. Rossetto, D. Bisi, A. Stocco, A. Chini, A. Pantellini, C. Lanzieri, A. Nanni, G. Meneghesso, and E. Zanoni, "Buffer Traps in Fe-Doped AlGaN/GaN HEMTs: Investigation of the Physical Properties Based on Pulsed and Transient Measurements," *IEEE Transactions on Electron Devices*, vol. 61, no. 12, pp. 4070–4077, Dec 2014.

[34] F. Alvarez, A. Alegra, and J. Colmenero, "Relationship between the time-domain Kohlrausch-Williams-Watts and frequency-domain Havriliak-Negami relaxation functions," *Phys. Rev. B*, vol. 44, pp. 7306–7312, Oct 1991. [Online]. Available: https://link.aps.org/doi/10.1103/PhysRevB.44.7306

[35] J. Pottage, private communication, 2018.

[36] T. Goorley, M. James, T. Booth, F. Brown, J. Bull, L. J. Cox, J. Durkee, J. Elson, M. Fensin, R. A. Forster, J. Hendricks, H. G. Hughes, R. Johns, B. Kiedrowski, R. Martz, S. Mashnik, G. McKinney, D. Pelowitz, R. Prael, J. Sweezy, L. Waters, T. Wilcox, and T. Zukaitis, "Initial MCNP6 Release Overview," *Nuclear Technology*, vol. 180, no. 3, pp. 298–315, 2012. [Online]. Available: https://doi.org/10.13182/NT11-135

[37] M. Norgett, M. Robinson, and I. Torrens, "A proposed method of calculating displacement dose rates," *Nuclear Engineering and Design*, vol. 33, no. 1, pp. 50 – 54, 1975. [Online]. Available: http://www.sciencedirect.com/science/article/pii/0029549375900357

[38] A. Johnston, *Reliability and Radiation Effects in Compound Semiconductors*. WORLD SCIENTIFIC, 2010. [Online]. Available: https://www.worldscientific.com/doi/abs/10.1142/7331

[39] T. Figielski, "Theory of carrier recombination at dislocations in germanium," *physica status solidi (b)*, vol. 6, no. 2, pp. 429–440, 1964. [Online]. Available: https://onlinelibrary.wiley.com/doi/abs/10.1002/pssb.19640060214

[40] P. Moens, A. Banerjee, M. J. Uren, M. Meneghini, S. Karboyan, I. Chatterjee, P. Vanmeerbeek, M. Csar, C. Liu, A. Salih, E. Zanoni, G. Meneghesso, M. Kuball, and M. Tack, "Impact of buffer leakage on intrinsic reliability of 650V AlGaN/GaN HEMTs," in *2015 IEEE International Electron Devices Meeting (IEDM)*, Dec 2015, pp. 35.2.1–35.2.4.

[41] M. J. Uren, D. G. Hayes, R. S. Balmer, D. J. Wallis, K. P. Hilton, J. O. Maclean, T. Martin, C. Roff, P. McGovern, J. Benedikt, and P. J. Tasker, "Control of Short-Channel Effects in GaN/AlGaN HFETs," in *2006 European Microwave Integrated Circuits Conference*, Sept 2006, pp. 65–68.

[42] M. J. Uren, J. Moreke, and M. Kuball, "Buffer Design to Minimize Current Collapse in GaN/AlGaN HFETs," *IEEE Transactions on Electron Devices*, vol. 59, no. 12, pp. 3327–3333, Dec 2012.

[43] H. J. von Bardeleben, J. L. Cantin, U. Gerstmann, A. Scholle, S. Greulich-Weber, E. Rauls, M. Landmann, W. G. Schmidt, A. Gentils, J. Botsoa, and M. F. Barthe, "Identification of the Nitrogen Split Interstitial $(\mathbf{N}-\mathbf{N})_{\mathbf{N}}$ in GaN," *Phys. Rev. Lett.*, vol. 109, p. 206402, Nov 2012. [Online]. Available: https://link.aps.org/doi/10.1103/PhysRevLett.109.206402

[44] D. C. Look, G. C. Farlow, P. J. Drevinsky, D. F. Bliss, and J. R. Sizelove, "On the nitrogen vacancy in GaN," *Applied Physics Letters*, vol. 83, no. 17, pp. 3525–3527, 2003. [Online]. Available: https://doi.org/10.1063/1.1623009

[45] J. Neugebauer and C. G. Van de Walle, "Atomic geometry and electronic structure of native defects in GaN," *Phys. Rev. B*, vol. 50, pp. 8067–8070, Sep 1994. [Online]. Available: https://link.aps.org/doi/10.1103/PhysRevB.50.8067